We are IntechOpen, the world's leading publisher of Open Access books Built by scientists, for scientists

4,800
Open access books available

122,000
International authors and editors

135M
Downloads

Our authors are among the

154
Countries delivered to

TOP 1%
most cited scientists

12.2%
Contributors from top 500 universities

CLARIVATE ANALYTICS BOOK CITATION INDEX INDEXED

WEB OF SCIENCE™

Selection of our books indexed in the Book Citation Index in Web of Science™ Core Collection (BKCI)

Interested in publishing with us?
Contact book.department@intechopen.com

Numbers displayed above are based on latest data collected.
For more information visit www.intechopen.com

11

Adaptive MIMO Channel Estimation Utilizing Modern Channel Codes

Patric Beinschob and Udo Zölzer
Helmut-Schmidt-Universität / Universität der Bundeswehr Hamburg
Germany

1. Introduction

For the ever increasing demand in high data rates the spectrum from 300 MHz to 3500 MHz gets crowded with radio, smartphones, and tablets and their competition for bandwidth. Regulators cannot realistically reduce demand, nor can they expand the overall supply.
A solution is seen in the uprising of Multiple-Input Multiple-Output (MIMO) communications. The sometimes poor spectral efficiency of established radio systems can be increased dramatically without expanding bandwidth and at reasonable signal power levels.
The term MIMO pays tribute to the fact that multiple antennas at sender and receiver are used in order to have spatially distributed access to the channel thus establishing additional degrees of freedom also referred to as spatial diversity. Spatial diversity can be used for solely transmit redundant symbols, e.g. Space-Time Block Codes, as well as the transmission of independent data streams via the spatial layers known as Spatial Multiplexing (SM). This mode is preferred over pure diversity usage as recently discussed by Lozano & Jindal (2010). However, the benefit comes at the price of increasing RF hardware expenses and geometry in case of many installed antennas which are the main reasons for reluctant implementations in the industry in former times. Additional algorithmic complexity at one point in the communication system is another reason. For SM mode, this is mainly in the receiver, where the independent data streams have to be separated in the detection process, leaving open questions in implementation issues of MIMO technologies in handheld devices.
For high data rate communications, MIMO in conjunction with Orthogonal Frequency Division Multiplexing (OFDM) offers the opportunity of exploiting broadband channels within reasonable algorithmic complexity measures (Bölcskei et al., 2002).
OFDM used as a standard technique in broadband modulation eases the equalization issue in MIMO broadband channels. For a given system with n_R receive antennas and n_T transmit antennas the MIMO channel is described by the $n_R \cdot n_T$ Single-Input Single-Output (SISO) spatial subchannels established between each transmit-receive antenna pair. For the sake of notation they are arranged in a so called channel matrix.
MIMO-OFDM modulation technique allows to consider the MIMO problem for each OFDM subcarrier separately. Thus, complexity is reduced by turning a $K \cdot n_R \times K \cdot n_T$ matrix inversion into K inversions of $n_R \times n_T$ matrices in the case of linear MIMO detection algorithms (Beinschob & Zölzer, 2010b).

For coherent receivers channel estimation is necessary. Recent advances in channel coding theory and feasibility of "turbo" principles and techniques led to new receiver designs, (Akhtman & Hanzo, 2007b; Hagenauer et al., 1996; Liu et al., 2003), optimal Detectors (Hochwald & ten Brink, 2003) and optimized codes for MIMO transmission (ten Brink et al., 2004) with the help of EXIT chart analysis (ten Brink, 2001) on LDPC Codes (Gallager, 1962; 1963), which were in turn rediscovered and revised by MacKay (1999).
Iterative decoding to approximate a posteriori probability (APP) information on the received data enhances the possibilities of classical adaptive signal processing approaches. On the other hand, MIMO Spatial Multiplexing APP detectors are very complex and only slowly convergent.
However, in practical systems large gaps between theoretically calculated capacity and realized data rates can be observed. The negative impact of imperfect channel knowledge on detection performance is significant (Dall'Anese et al., 2009). Those errors are especially high in mobile scenarios. Constraints on the amount of reference symbols that use exclusive bandwidth is natural. So, as a solution decision-directed techniques in adaptive channel estimators are considered that utilize information from the obligatory forward error correction in order to increase the channel estimation accuracy.
Our approach focuses on a minimization of pilot symbols. Therefore, only a small initial training preamble is send followed by data symbols only as shown in Fig. 2. The use of distributed pilot symbols, a common approach for slow fading channels – also employed in LTE, is avoided that way. The application of adaptive filtering in combination with decision-directed techniques is shown here to provide the necessary update of the channel state information in time varying scenarios like mobile receivers.
The discussed channel estimation techniques aim to add only reasonable complexity, so non-iterative approaches are considered. It is non-iterative in the sense that no a priori feedback is given to the detector. Hence it is suited for low latency applications, too. Channel estimates are readily available at OFDM symbol rate as well as the decoded data bits.
The chapter is organized as follows. The basic system model is presented in the next section, with a discussion of channel characterization and used pilot symbols for minimum training length in Section 2.3. Common approaches to channel estimation with minimum training length are reviewed in Section 3. The receiver structure we focus on is presented in Section 4. Results of conducted numerical experiments are discussed in Section 5.
Notation is used as follows. Bold face capital letters denote matrices, column vectors are typed in bold small letters. The operator $(\cdot)^{\mathsf{H}}$ applies complex-conjugate transposition to a vector or matrix. Time domain signals carry the check accent, e. g. $\check{x}$, in order to distinguish them from their frequency domain counterpart.

2. System model

2.1 Bit-interleaved coded MIMO-OFDM

A multiple antenna systems is represented as a time discrete model in a multi-path channel in the following fashion: The vector of received values $\check{\mathbf{r}}$ at the time sample m of a MIMO system is the superposition of $L \cdot n_T$ previously sent samples and the current n_T samples, where $L+1$ is the length of the sampled channel impulse response. It is given by

$$\check{\mathbf{r}}[m] = \sqrt{E_s} \sum_{l=0}^{L} \check{\mathbf{H}}[l, m] \cdot \check{\mathbf{s}}[m-l] + \sigma_w \check{\mathbf{w}}[m], \tag{1}$$

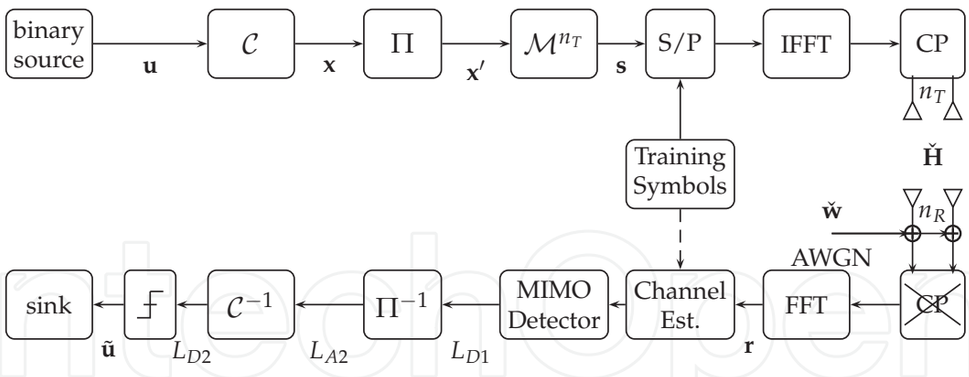

Fig. 1. MIMO-OFDM system with standard receiver processing.

where $\check{\mathbf{s}}[m]$ denotes the current vector of symbols of each of the transmit antenna, $\check{\mathbf{w}}$ is an identically, independently distributed (iid) additive white Gaussian noise term and $\check{\mathbf{H}}[l,m]$ is the MIMO channel matrix in delay and time domain, indexed with l respectively m. It is therefore the MIMO Channel Impulse Response per time sample m. The past sent samples are denoted by $\check{\mathbf{s}}[m-l]$, for $l \neq 0, l \leq L$. The data symbols of the K subcarriers are modulated by an inverse Fast Fourier Transform (IFFT). In simulations every value corresponding to a transmit antenna of the resulting vectors is transmitted using the formula above.
The MIMO-OFDM system model in frequency domain is described by

$$\mathbf{r}[n,k] = \sqrt{E_s}\mathbf{H}[n,k] \cdot \mathbf{s}[n,k] + \sigma_w \mathbf{w}[n,k], \tag{2}$$

where n denotes the time index of an OFDM symbol and k its subcarrier index, where K is the total number of subcarriers. As a Signal-to-noise measure E_b/N_0 is defined with noise variance given by $\sigma_w^2 = N_0$, where N_0 is the spectral noise power density in equivalent base band domain and with the energy per (QAM) symbol

$$E_s = R_c \cdot \kappa \cdot E_b, \tag{3}$$

where R_c is the code rate and κ bits per QAM symbol.
The receive vector $\mathbf{r}[n,k]$ and noise vector $\mathbf{w}[n,k]$ are of dimension $n_R \times 1$, the send vector $\mathbf{s}[n,k]$ of $n_T \times 1$ and the matrix $\mathbf{H}[n,k]$ of $n_R \times n_T$, at which n_R is the number of transmit antennas. The entries of $\mathbf{w}[n,k]$ are complex circular-symmetric Gaussian distributed random variables where $w_r[n,k] \sim \mathcal{CN}(0,1), r = 1,\ldots,n_R$ holds.
A perfect synchronization and total avoidance of block interference is assumed, so the OFDM cyclic prefix L_{cp} is longer than the discrete maximum path delay denoted by the channel order L, hence $L_{cp} > L$. The system overview is depicted in Fig. 1.
The MIMO-OFDM sent symbols are separately bit-interleaved LDPC codewords, where the EXIT chart of the employed LDPC code is shown in Fig. 4. The sender limits the codeword and interleaver length to the number of available bits in a MIMO-OFDM symbol n that is $n_T \cdot K \cdot \kappa$. The data symbols are drawn from an M-order QAM modulation alphabet $\mathbb{S}$. The mapping, denoted by $\mathcal{M}\{\cdot\}$, modulates $\kappa = \log_2 M$ bits to a QAM symbol. This is done consecutively for all n_T sent streams/layers hence the notation $\mathcal{M}^{n_T}\{\cdot\}$. The QAM constellations are considered unit power-normalized to simplify notation. At the receiver, the Log-Likelihood Ratios (LLRs) can be de-interleaved and LDPC decoded at once after reception, FFT and MIMO detection, which yields the approximated a-posteriori LLRs $L_{D2}[n]$

out of the received symbols:

$$L_{D2}[n] = \mathcal{C}^{-1}\left\{\Pi^{-1}\{L_{D1}[n]\}\right\}. \tag{4}$$

Scrutinizing the sign of $L_{D2}[n]$ yields the most probable sent codeword $\mathbf{y}[n]$. Finally, the transmitted information bits $\tilde{\mathbf{u}}[n]$ are recovered by discarding the redundancy bits in $\mathbf{y}[n]$.

2.2 MIMO channel model

Typically a (static) MIMO channel realization can be modeled by drawing the coefficients $\check{H}_{r,t}$ independently from a complex circular-symmetric Gaussian distribution.

$$\check{H}_{r,t}[l] \sim \mathcal{CN}\left(0, \frac{1}{(L+1)}\right), r = 1, \ldots, n_R,\ t = 1, \ldots, n_T. \tag{5}$$

Doing so for all $L+1$-multi-path time-domain MIMO channel coefficients implies a constant power delay profile for all spatial subchannels.

Of course, in mobile communication time-variant channel behaviour is expected. For multiple antennas systems in urban environments we have array size limitations thus small distances between the colocated antennas which renders the assumption of i.i.d. channel coefficients unrealistic. In order to conduct realistic simulations the 3GPP developed a Spatial Channel Model (SCM) suitable to test algorithms supporting mobile MIMO systems in macro- or micro urban scenarios (*Spatial channel model for Multiple Input Multiple Output (MIMO) simulations*, 2008).

Mobile receivers experiences velocity-dependent Doppler frequency shifts in components of the superposed received signal. For an OFDM system the consequence might be a gradually loss of orthogonality of the subcarriers which results in Intercarrier Interference (ICI).

Considering a wireless OFDM system at carrier frequency f_0 with OFDM symbol duration $T_{\mathrm{OFDM}} = (K + L_{\mathrm{cp}})/f_{\mathrm{S}}$ in seconds (f_{S} being the sampling rate), a maximum Doppler frequency in Hertz for a given mobile station's relative radial velocity of v_{MS} is given by

$$f_{\mathrm{D}} = \frac{v_{\mathrm{MS}}}{c} \cdot f_0, \tag{6}$$

with c being the speed of light. As a measure in OFDM systems the normalized Doppler frequency is of more interest because of its independence of the system parameters K and L_{cp}:

$$f_{\mathrm{D,n}} = f_{\mathrm{D}} \cdot T_{\mathrm{OFDM}}. \tag{7}$$

As a rule of thumb, significant ICI appears if $f_{\mathrm{D,n}} > 5 \times 10^{-3}$. Associated with f_{D} a coherence time interval T_{coh} can be defined as by Proakis & Salehi (1994)

$$T_{\mathrm{coh}} = \frac{1}{2f_{\mathrm{D}}}. \tag{8}$$

2.3 Training symbol design

Training symbols must be carefully chosen in order to maximize the signal-to-noise ratio during estimation. In OFDM systems, it is important to design training symbols that have low peak-to-average-power ratio (PAPR) in time-domain. Spatial orthogonality should be preserved in frequency-domain for the different transmit antennas. As basic construction of

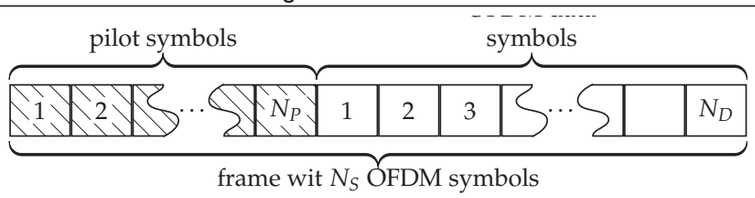

Fig. 2. Frame structure for proposed MIMO-OFDM RLS-DDCE with preamble length N_P symbols with $N_p \geq n_T$

orthogonal sequences Frank-Zadoff-Chu (FZC) sequences $\mathbf{p}_t,\ t = 1, \ldots, n_T$ are chosen (Chu, 1972):

$$\mathbf{p}_i^{\mathsf{H}} \mathbf{p}_j = \begin{cases} 1 & \text{for} \quad i = j \\ 0 & \text{for} \quad i \neq j. \end{cases} \tag{9}$$

It is a special property of FZC sequences that the sequence $\mathbf{p}_j$ is yielded by cyclic shifting of $\mathbf{p}_i$ by $j - i$ positions. The sequences are inserted over time and a subcarrier-specific phase to lower the PAPR is added, e.g. for the first sequence

$$p_1[n,k] = \mathrm{e}^{j\pi M'(n-1)^2/n_T + \varphi[k]}, \quad n = 1, \ldots, n_T. \tag{10}$$

The phases are taken from another FZC sequence of length K:

$$\varphi[k] = \pi M''(k-1)^2/K, \quad k = 1, \ldots, K. \tag{11}$$

M' and M'' are prime numbers less or equal to $n_T + 2$ and $K + 2$, respectively. Each antenna t sends its $p_t[n,k]$ as training preamble at the beginning of the frame. Construction is possible for all length of n_T and K and leads to time and frequency domain signals with minimum PAPR.
The underlying frame structure provides a training sequence at the beginning of each frame as shown in Fig. 2.

3. Decision-directed channel estimation techniques

From Eq. (2) it is clear that estimating the channel matrix $\mathbf{H}$ is difficult even if the send vector is known due to the rank-deficit of the problem. Therefore, for the estimate it needs a scheme that efficiently exploits all given diversities: time, frequency and space. A promising approach is given by Akhtman & Hanzo (2007a), that proposed an adaptive channel estimation structure. In the first step, a spatial auto- and crosscorrelation estimator is employed for each subcarrier individually. Originally, a further stage for dimension reduction – using the PAST scheme – is employed. It is not considered here in order to eliminate further influence of parameters and to separate the effects. However, in order to exploit the correlation of adjacent subcarriers, LDPC codewords are interleaved over spatial streams and subcarriers. So the structure is enhanced by the usage of short yet powerful LDPC codes, employing the belief propagation decoder to approximate posteriori information on the send symbol which are used in the decision-feedback processing. Deep fading occurring occasionally on individual subcarriers would result in low LLRs, which are less trusted in belief propagation decoding. But through message-passing their information is recovered from the other connected nodes. By simple parity or syndrome check – a property which LDPC codes inherit from the family

of linear block codes –, a reliable and readily available criterion is given to control the overall decision feedback of the channel estimator.

3.1 Recursive least squares estimation

Due to the unknown error distribution the channel estimation is often formulated as a *Least Squares* problem: Find a channel matrix estimate $\tilde{\mathbf{H}}[n]$ at the symbol n that projects the send vector $\mathbf{s}[n]$ in the receive vector space, such that the euclidean distance to the actual received vector $\mathbf{r}[n]$ is be minimized:

$$J_{RLS}[n] = \sum_{m=1}^{n} \xi^{n-m} \mathbf{e}^{\mathsf{H}}[m,n]\mathbf{e}[m,n], \tag{12}$$

with the error signal

$$\mathbf{e}[m,n] = \mathbf{r}[m] - \tilde{\mathbf{H}}[n] \cdot \mathbf{s}[m]. \tag{13}$$

This classic approach yields good results with increasing samples if the unknown channel matrix $\mathbf{H}$ is constant. For time-variant channels old samples will increase the estimation error as the channel coefficients keep changing slowly. To gain adaptivity a "forgetting" factor $0 < \xi \leq 1$ is introduced, that applies a weighting depending on the sample index such that newer sample have stronger influence on the estimate than older ones. An exponential decreasing weighting has some implementation qualities that will be pointed out in the following.
A LS channel estimate of the channel matrix $\mathbf{H}$ is yielded by

$$\tilde{\mathbf{H}}[n] = (\tilde{\mathbf{\Phi}}^{-1}[n]\tilde{\mathbf{\Theta}}[n])^{\mathsf{H}}. \tag{14}$$

with the estimated spatial auto- and cross-correlation matrices based on

$$\tilde{\mathbf{\Phi}}[n] = \sum_{m=1}^{n} \xi^{n-m} \mathbf{s}[m]\mathbf{s}^{\mathsf{H}}[m] = \xi\tilde{\mathbf{\Phi}}[n-1] + \mathbf{s}[n]\mathbf{s}^{\mathsf{H}}[n], \tag{15}$$

and

$$\tilde{\mathbf{\Theta}}[n] = \sum_{m=1}^{n} \xi^{n-m} \mathbf{s}[m]\mathbf{r}^{\mathsf{H}}[m] = \xi\tilde{\mathbf{\Theta}}[n-1] + \mathbf{s}[n]\mathbf{r}^{\mathsf{H}}[n]. \tag{16}$$

The known pilot symbols are used as substitutes for the sent vectors $\mathbf{s}[n,k]$ if $n \leq N_p$, otherwise the decision-feedback is used. A $\xi := 1$ is optimal if a static channel is considered because the estimation error keeps decreasing with increasing n as long as there are no false decisions in the feedback.
If only pilot symbols are utilized, no further information is available beyond the training and the channel estimates need to be used for the rest of the frame. For $\xi = 1.0$, this technique is referred as ordinary Least-Squares (LS) Channel Estimation in the following.
Due to the orthogonal designed pilot symbols, the matrices $\tilde{\mathbf{H}}[n,k]$ have full condition at $n = n_T$ yet they are superposed by noise.

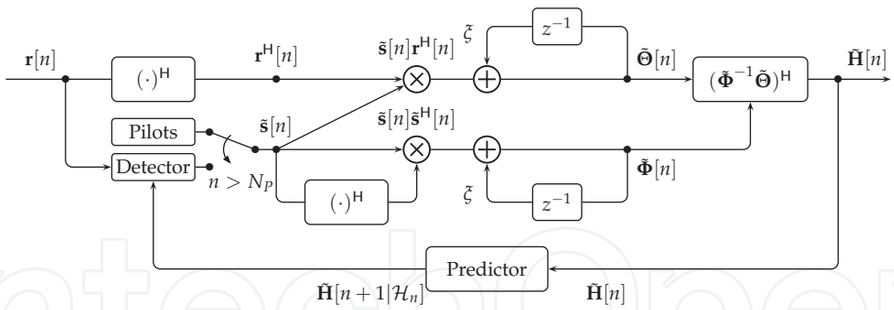

Fig. 3. Signal Flow diagram RLS algorithm.

3.2 Algorithmic structure

In Fig. 3 the algorithmic structure is shown. After N_P pilots of constant-energy type (Chu, 1972), the output of the MIMO detector is used instead of the known pilots in order to estimate the spatial auto- and cross-correlation matrices $\tilde{\mathbf{\Phi}}$ resp. $\tilde{\mathbf{\Theta}}$ independently per subcarrier. Averaging is performed in the recursive part of the structure and weighting with a forgetting factor ξ is applied to suppress older samples and adapt to newer ones. The detector uses the channel estimate for detection. To mitigate the effect of outdating CSI, a predictor is employed that tracks the time-variant MIMO channel $\mathbf{H}$ and calculates an prediction $\tilde{\mathbf{H}}[n+1|\mathcal{H}_n]$. Through the immediately detection of data this algorithm is in principle suited to low delay applications as pointed out by Beinschob & Zölzer (2010a).

3.3 Decision feedback

3.3.1 Hard decision feedback

Further information on the channel can be acquired by using the detection output in Eq. (15) and (16), i. e. estimated sent vectors as proposed in Akhtman & Hanzo (2007a),

$$\tilde{\mathbf{s}}[n] = \mathcal{M}^{n_T}\{\mathrm{sgn}\{L_{D1}[n]\}\}, \quad \forall n > N_P. \tag{17}$$

The algorithm is illustrated in Fig. 3. This is referred to as decision-directed channel estimation. It is prone to error propagation since incorrect decisions increases the channel estimation error, which in return increases the probability of incorrect decisions. Feedback with incorrect symbols in an early stage of the frame renders the channel estimate for the rest completely useless.

3.3.2 Soft decision feedback

In contrast to Eq. (17) hard decision, the sent MIMO-OFDM symbols can be estimated by evaluating the symbol expectation values (Glavieux et al., 1997) based on the detection probabilities p associated with $L_{D1}[n]$:

$$\tilde{s}_t[n] = \mathrm{E}\{s_t\} = \sum_{c \in \mathbb{S}} c \cdot p(\tilde{s}_t[n] = c), \quad \forall t. \tag{18}$$

The reconstructed sent vectors can be applied in Eq. (15) and (16). The *soft* symbol value is determined by the reliability of LLRs, i. e. magnitude. If low LLRs occur Eq. (18) evaluates to near zero, which can lead to stability problems in Eq. (14) for $\xi < 1$ due to exponentially decreasing values in $\tilde{\mathbf{\Theta}}$. This scheme is referred to as soft-decision RLS (RLSsd).

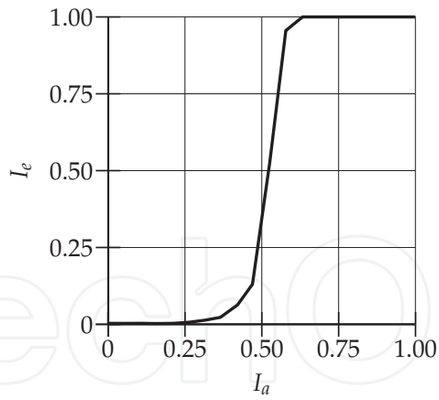

Fig. 4. Extrinsic mutual information transfer (EXIT) chart of used LDPC code 1024 bit length constructed with edge distributions from Richardson et al. (2001).

4. Proposed receiver structure

4.1 Conditioned a posteriori decision-feedback

Following the decision-feedback strategy of Eq. (17) the estimator has no information about the certainty of the feedback. Using soft-decision feedback the estimated sent vectors still contain the noise from detection stage. The developing of the channel estimation error $\varepsilon[n]$ can be very roughly modeled as follows:

$$\varepsilon[n] = \frac{\sigma_e^2}{n} + N_e \sigma_c^2 \tag{19}$$

On one hand the channel estimation error decreases with growing n through the averaging effect, where the error energy per gained channel estimate sample due to noise and spatial interference is denoted σ_e^2. On the other hand an incorrect decision directly adds the error energy σ_c^2, which contains the energy of a false channel estimate plus noise and interference. The cost of incorrect decisions are unequally higher as the benefit of another correct sample for averaging, especially for higher n. Hence an incorrect decision should be avoided even at the price of low number of samples to average.

By utilizing channel decoder L_{D2} information at the decision stage, the feedback of incorrect decisions can be avoided. For time-invariant channels the weighting factor is set to $\xi := 1.0$ because an update via Eq. (15) and (16) is applied only if the codeword associated with the MIMO-OFDM symbol is successfully decoded. For linear block codes this is indicated by the syndrome vector

$$\boldsymbol{\gamma}[n] = \mathbf{A} \cdot \mathbf{y}[n]. \tag{20}$$

The parity check matrix is denoted $\mathbf{A}$, the received codeword is

$$\mathbf{y}[n] = \operatorname{sgn}\{L_{D2}[n]\}. \tag{21}$$

Note that Eq. (20) and (21) are evaluated in most LDPC decoder implementations as break criterion for the iteration process. So, if the decoder signals $\|\boldsymbol{\gamma}[n]\|_{\mathrm{H}} = 0$, where $\|\cdot\|_{\mathrm{H}}$ denotes the Hamming distance, the sent vectors in Eq. (15) and (16) are substituted by

$$\{\tilde{\mathbf{s}}[k,n]\}_{k=1}^{K} = \mathcal{M}^{n_T}\{\Pi\{\mathbf{y}[n]\}\}, \tag{22}$$

using the property of the systematic linear block code which renders additional re-encoding unnecessary. Because of the high codeword distance it is unlikely that the codeword $\mathbf{y}[n]$ contains undetected errors or being another valid codeword. However, this is a source of the algorithm's residual errors. In the case $\|\boldsymbol{\gamma}[n]\|_{\mathrm{H}} \neq 0$, no update is performed instead the former channel estimate is assumed to be still valid:

$$\tilde{\mathbf{H}}[n,k] := \tilde{\mathbf{H}}[n-1,k], \tag{23}$$

which can be seen as a simple zero order hold prediction.
As pointed out with the rough model in Eq. (19), feedback of erroneous data increases the estimation error over-proportional compared to the benefit of another sample to average. However, for valid codewords this approach leads to an extension of the training length due to the usage of data symbols as virtual pilots. The benefit is especially large at the beginning of a frame, directly after the end of pilots. There, the channel estimate error is still high and therefore the probability of false detection is high. The proposed scheme is referred in the following as Conditional Feedback (RLSCF).
The estimated channel matrix $\tilde{\mathbf{H}}$ is used in the MIMO detection, where LLR channel values L_{D1} are determined per OFDM symbol and subcarrier on a Maximum Likelihood (ML) basis:

$$L_{D1}(t,\nu) = \frac{1}{\sigma_{\tilde{w}}^2}\left(\min_{\mathbf{s}\in\mathcal{S}^{\nu,+1}} \|\mathbf{r}-\mathbf{H}\mathbf{s}\| - \min_{\mathbf{s}\in\mathcal{S}^{\nu,-1}} \|\mathbf{r}-\mathbf{H}\mathbf{s}\|\right), \tag{24}$$

where $\mathcal{S}^{\nu,+1}$ denotes the set of all possible send vectors that ν-th bit is $+1$, $|\mathcal{S}| = |\mathcal{M}|^{n_T}$ and considering unit-power constellations. Of course, ML-approximating detection algorithms, i. e. List Sphere Decoder (Hochwald & ten Brink, 2003) can be applied here as well. $\sigma_{\tilde{w}}^2$ is the channel noise power which is often assumed to be known at the receiver.

4.2 Complexity discussion

Most of the proposed processing is straight-forward: OFDM demodulation, subcarrierwise MIMO detection, de-interleaving and LDPC decoding has to be done in any coherent MIMO receiver coping with multipath channels. The additional complexity comes from an interleaver and a MIMO symbol mapper in the channel estimation feedback chain. In the soft decision case there is more computing power necessary with only marginal performance gains compared to the hard decision technique. However, the main contribution to complexity raises in the channel estimation itself for possibly updating the channel estimation at each OFDM symbol if the SNR is sufficient high and the channel decoder is successful decoding the codeword. In this case the LDPC decoder that is aware of a valid codeword and stops the iteration, needs less internal iterations so there is a shift in complexity from the decoder to the channel estimator.
The estimation procedure can be further simplified by help of the matrix inversion lemma to avoid explicit inversion of the autocorrelation matrix. The resulting algorithm is described in Beinschob et al. (2009).

5. Numerical experiments

5.1 Channel estimation accuracy & system performance

In a MIMO system, the detection depends on the received vector $\mathbf{r}$ and channel matrix $\mathbf{H}$ (Hochwald & ten Brink, 2003). In real scenarios the channel matrix is not available and an

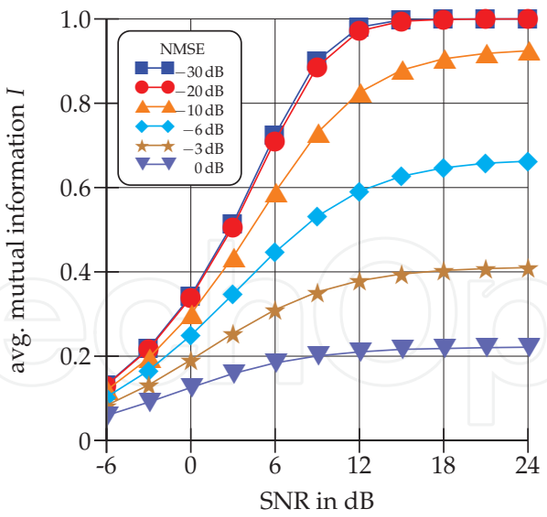

Fig. 5. Average Mutual Information of a MIMO 4 × 4 Spatial Multiplexing with 4-QAM modulation and different levels of Channel Estimation Errors in terms of NMSE.

estimate $\tilde{\mathbf{H}}$ is used instead. To evaluate the quality of the detector output, which is of most importance for the decision-directed scheme, the mutual information of the gained (uncoded) LLRs is used (ten Brink, 1999). The performance degradation in presence of estimation errors is assessed by modelling a channel estimate as follows:

$$\tilde{\mathbf{H}} = \mathbf{H} + \Delta\mathbf{H}, \tag{25}$$

where $H_{r,t} \in \mathcal{CN}(0,1)$ are the i.i.d. MIMO Rayleigh Fading channel coefficients and elements of $\Delta\mathbf{H}$ are i.i.d. circular symmetric complex Gaussian random variables with error variance σ_e^2. This also covers to some extent the case of mobility induced interference because the ICI leads to additional noise in the Frequency Domain as pointed out by Russell & Stuber (1995). As a measure for the estimation error the normalized mean squared error is defined as

$$\text{NMSE} = \frac{\sum_{t=1}^{n_T}\sum_{r=1}^{n_R}\left|H_{r,t} - \tilde{H}_{r,t}\right|^2}{\sum_{t=1}^{n_T}\sum_{r=1}^{n_R}\left|H_{r,t}\right|^2}. \tag{26}$$

So, the channel capacity for discrete input alphabet (4-QAM) and continuous channel output is shown in Fig. 5.
In general, the capacity increases with SNR and with decreasing channel estimation NMSE. However, a saturation of I over SNR can be observed: With increasing estimation error the maximum level of mutual information I decreases.
At minimum, a NMSE of −6 dB to −10 dB is necessary for a half-rate coded system to work properly. Below −20 dB NMSE there is no significant difference in the system's performance using either the channel estimate or the actual channel matrix.

5.2 System level simulations for time-invariant channels

In Tab. 1 the system parameters are given for the experiments described in this section. For the

$n_T \times n_R$	4×4
Detector	Maximum Likelihood
OFDM Subcarriers	128
Modulation	4-QAM
MIMO-OFDM symbols per frame	516
bandwidth efficiency	≈3.8 bit/s/Hz
Pilot symbols per antenna	4 (0.8%)
Channel Model	$\mathcal{CN}(0,1)$
channel multi-path order L	6
OFDM cyclic prefix L_{cp}	7
channel coherence time T_c	> frame length
LDPC code design rate R_c	1/2
codeword & interleaver length	1024 bit

Table 1. Simulation parameters for time-invariant channel

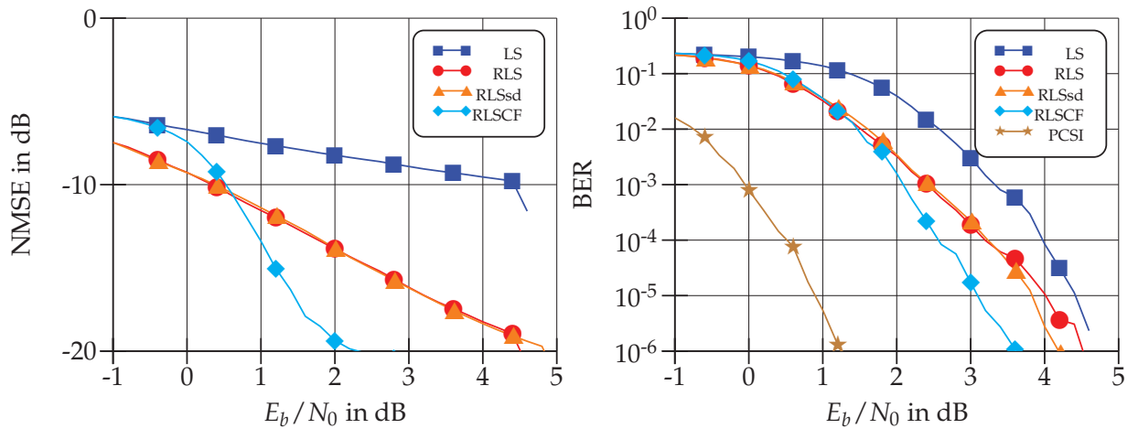

Fig. 6. BER and NMSE for the discussed schemes evaluated by Monte Carlo simulations using time-invariant channels with system parameters defined in Tab. 1.

BER/NMSE system level simulations a Maximum Likelihood bit detector with LLR output, combined with a short LDPC code of 1024 bit length, inserted in an MIMO-OFDM symbol, were used. Simulations were conducted for the case of minimum pilot symbol length $N_P = n_T$. The proposed channel estimation (RLSCF) was compared to the ordinary LS approach, the hard/soft-decision feedback approach by Eq. (17) (RLS resp. RLSsd) and detection with perfect channel state information (PCSI). Independent block-fading MIMO channel realization were generated which were frequency-selective but time-invariant during the frame, see Eq. (5).

The channel estimation error is assessed in terms of normalized mean squared error (NMSE), shown in Fig. 6. Least Squares channel estimation using only the available short training symbol sequence was inferior to the discussed decision-directed schemes. An improvement of RLS/RLSsd over LS can be observed. With increasing E_b/N_0 more correct feedback was available and decreased the NMSE, as reflected by the stronger slope of the RLS/RLSsd curve. RLS and RLSsd performed equally on average. The proposed method, RLSCF, performed worse than RLS/RLSsd for low E_b/N_0. This is because the feedback is limited to valid codewords only, which occurred seldom. So the averaging effect is almost as limited as in

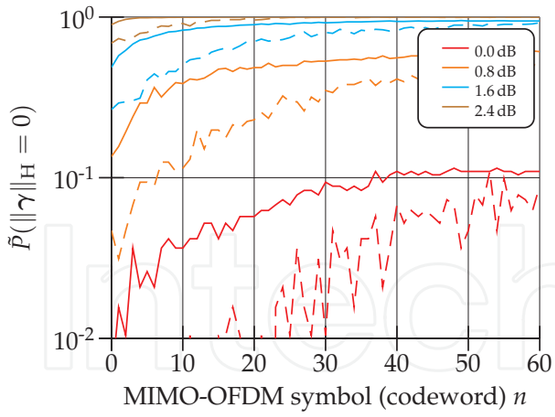

(a) Rate of successful decoding as indicated by $\|\boldsymbol{\gamma}\|_H = 0$, for different channel E_b/N_0, comparing proposed RLSCF (solid) and RLS (dashed lines).

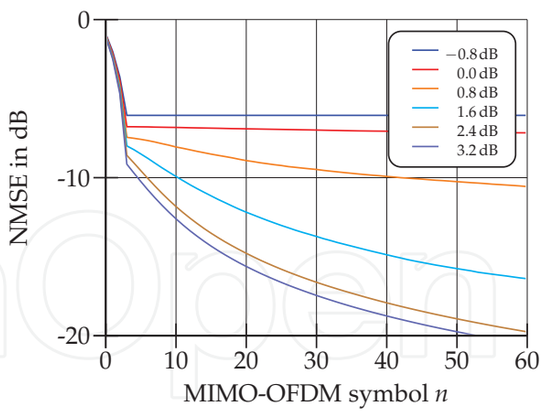

(b) NMSE per MIMO-OFDM symbol (time) index n and selected E_b/N_0.

Fig. 7. Developing of NMSE over time resp. OFDM symbol index for RLSCF scheme (multiple frames and channel realizations averaged).

the LS case. Beyond 1 dB E_b/N_0 RLSCF performed better than RLS/RLSsd because it can be deduced that there were plenty of virtual pilots, as depicted in Fig. 7(a).
There the rate of indicated successful decoding over MIMO-OFDM symbol index n is shown. Especially in the beginning of the frame a higher rate of successful decoding could be achieved with the proposed channel estimator RLSCF. This led to more virtual pilots and improved NMSE depicted in Fig. 7(b).
The developing channel estimation error in terms of normalized mean square error (NMSE) can be seen for different E_b/N_0 in Fig. 7(b). Due to the short training the channel estimation error is rather high at the beginning of the frame and decreases with $\propto 1/n$ if the SNR is sufficient so that the decoder could deliver successful decoded feedback. This the case for E_b/N_0 above $\approx$1 dB, below only insignificant improvements could be realized. This threshold is a property of the LDPC code, which is visualized in the EXIT chart in Fig. 4. Only if the input information exceeds the threshold successful decoding is possible. This means for the proposed scheme, for $E_b/N_0 < 1$ dB only marginal gains could to realized compared to LS, where as for higher values significant improvements in terms of NMSE were achieved.
For completeness the resultant system Bit Error Rate (BER) of the conducted simulations are shown in Fig. 6. For reference a curve for detection with perfect channel state information (PCSI) is shown, too. On the right hand side the detection based on Least Squares channel estimation using only the available training symbols is shown. The performances of the discussed decision-directed schemes were in between, reflecting the same tendency as the NMSE plot in Fig. 6. Here for higher E_b/N_0 RLSsd performed marginal superior. By using detection-based decision-directed strategies it was possible to decrease the BER but due to erroneous feedback it was rather small. For the proposed conditional a-posteriori feedback (RLSCF) a gain of 1 dB could be achieved. The gap of 2 dB to the decoding with perfect channel knowledge can be explained with the limited codeword distance of the short LDPC code used.

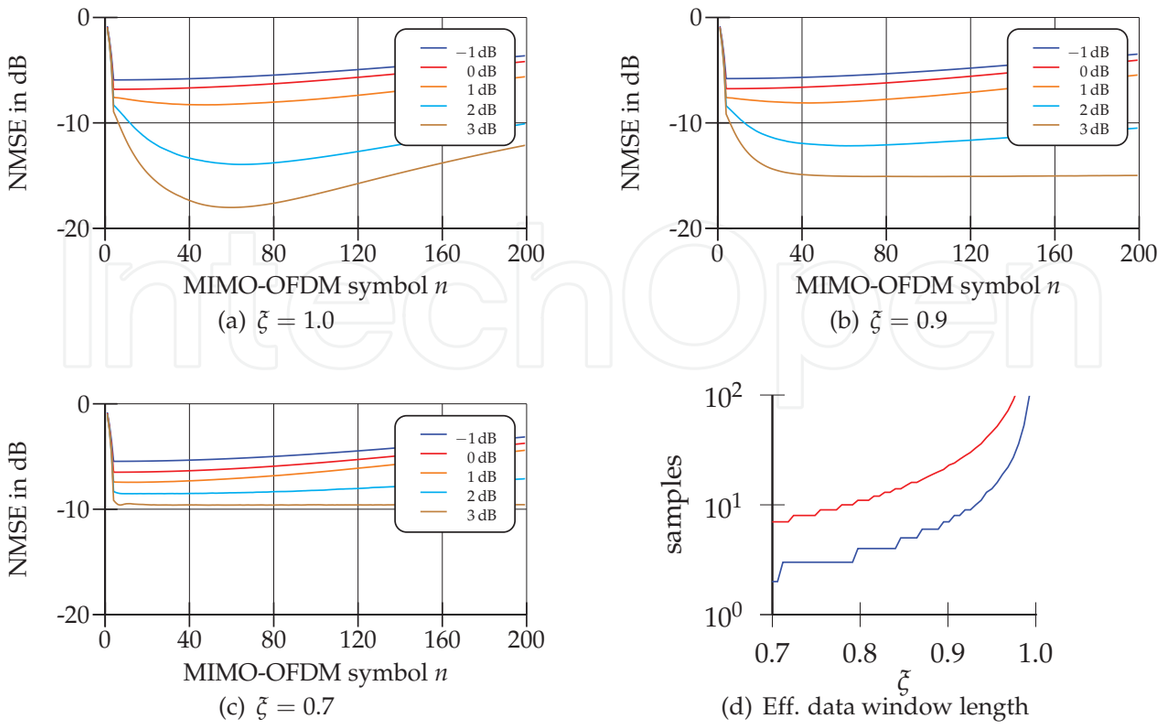

Fig. 8. Comparison of adaptivity on time variant channels (10 m/s) of channel code constraint feedback (RLSCF) for different forgetting factors ξ, also shown the effective data window length of forgetting factor in samples for coherence time (3 dB - blue line) and 10 dB (red line).

5.3 Simulations for 3GPP channels

To evaluate algorithms for real application a realistic channel model is needed. In particular the mobility component for the multipath MIMO case must be modelled very well. For this purpose the 3GPP Spatial Channel Model (*Spatial channel model for Multiple Input Multiple Output (MIMO) simulations*, 2008) is applied here.

5.3.1 Time adaptivity analysis

Fig. 8 illustrates the adaptivity of the DDCE structure depicted in Fig. 3. Clearly visible is the balance of the forgetting factor ξ which was too inflexible if set to $\xi = 1.0$ then the algorithm failed to track the channel well, although the NMSE became very low after 60 symbols. On the other hand, if set to $\xi = 0.7$, even for 3 dB E_b/N_0 the NMSE was insufficient for reliable transmissions. So a higher E_b/N_0 is needed for lower forgetting factors and thus higher adaptivity to achieve the same system performance for mobility scenarios.

5.3.2 System level results

For the 3GPP channel simulations RLSCF-based DDCE schemes were investigated through Monte Carlo simulations due to the lack of analytical tools to this kind of detection and channel estimation feedback structure. A Point-to-Point link is considered with Signal-to-noise-based assessment instead of range-dependence. Independent channel realization were generated for each frame. A frame consisted of 516 MIMO-OFDM symbols

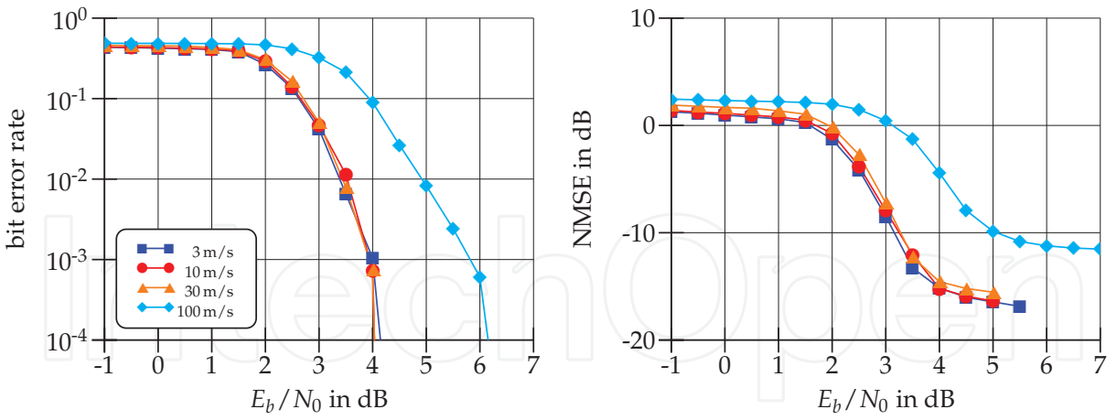

(a) RLS forgetting factor $\xi = 0.9$

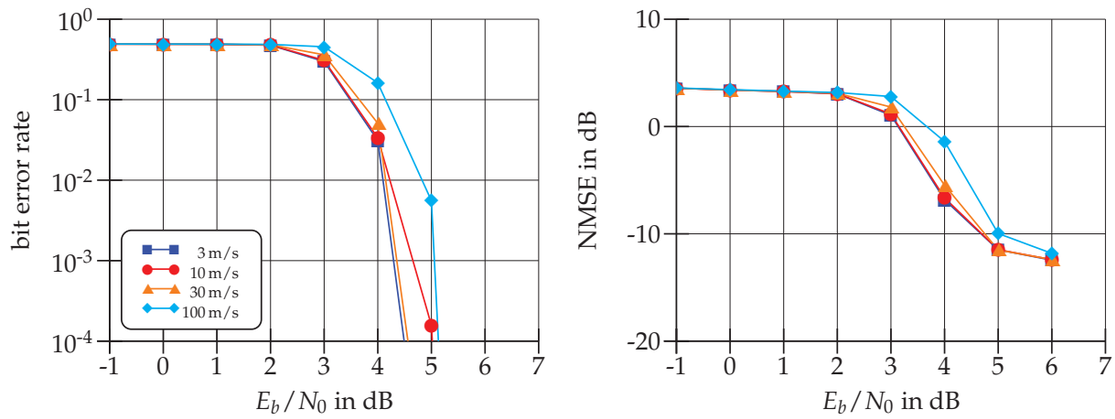

(b) RLS forgetting factor $\xi = 0.7$

Fig. 9. On the left BER vs. E_b/N_0 for burst transmissions in time variant channels with minimal pilot length $N_P = n_T$ for 4×4 MIMO, on the right channel estimation error in NMSE (same legend as left hand).

constructed by modulating uncorrelated random bits. Transmissions were simulated until either 3×10^5 bit were transmitted or at least 200 frames errors were encountered per E_b/N_0 and velocity setting. The E_b/N_0 level was not further increased if in 3×10^5 bit no bit errors occurred after the channel decoder.

As seen from the results for time-invariant channels, RLSCF clearly gave best results in terms of BER/NMSE. As already mentioned, in order to maximize the bandwidth efficiency, we focus on having minimal number of pilot symbols, that is when $N_P = n_T$. So for the 4×4 MIMO system we employed 4 pilot tones per subcarrier and spatial stream, having a pilot rate of 0.8 %.

As pointed out in the previous section, it is obvious that the forgetting factor has influence on the NMSE performance due to the averaging effect. Left of Fig. 9 shows the BER of RLSCF for increasing velocities of the mobile terminal. But it is difficult to predict whether an improved adaptivity on time-variant channels pays off the lost samples for the averaging. Simulation results for comparative study can be seen in Fig. 9. For a forgetting factor of $\xi = 0.9$ (see

Fig. 9(a)), it can be seen that performance degradation started somewhere above 30 m/s. For lower velocities virtually error-free reception was observed for E_b/N_0 above 4.5 dB. In the case of very high velocities, strong variations in the channel occurred which led to an increased channel estimation error in terms of NMSE.
In comparison with the forgetting factor setting of $\xi = 0.7$ (see Fig. 9(b)), we observed a general rise in NMSE due to the smaller effective data window length, which in turn leads to a worse BER. An exception is the highest velocity, which seemed unaffected by the shorter data window size in terms of NMSE. The same NMSE performance for $\xi = 0.7$ and $\xi = 0.9$ could be achieved. We can deduce that for 100 m/s during the longer data window size the channel changed significantly and therefore the additional samples were of no use for the averaging process. While the NMSE seemed unaffected there was influence visible in the BER results. A shorter window length led to a earlier E_b/N_0 level of virtually error-free transmission, about 1 dB.

6. Conclusion

A promising structure to perform channel estimation for a multitude of channel scenarios using minimum amount of pilots enhanced by decision-directed techniques is presented. Through the employment of modern channel coding in the feedback the algorithm is capable to improve the channel estimate thus decreasing the estimation error beyond the pilot sequence only by using data symbols as virtual pilots. Optimal tracking of time-variant channels is still an open problem, although good results can be achieved by regarding influence length resp. coherence time of the channel and choosing the forgetting factor ξ appropriately. However, in many practical cases lower velocities are encountered which can be exploited quite well with a high forgetting factor like $\xi = 0.9$ as shown in the results. For highest velocities we loose about 1 dB in E_b/N_0 but gain in NMSE and BER for the lower velocities. There is a general trade-off between good system performance in low E_b/N_0 or high velocities scenarios where the usable data window size gets too small for significant averaging gains in the channel estimation.

7. References

Akhtman, J. & Hanzo, L. (2007a). Advanced channel estimation for MIMO-OFDM in realistic channel conditions, *IEEE International Conference on Communications, ICC '07* pp. 2528–2533.

Akhtman, J. & Hanzo, L. (2007b). Iterative receiver architectures for MIMO-OFDM, *IEEE Wireless Communications and Networking Conference, WCNC*, pp. 825–829.

Beinschob, P., Lieberei, M. & Zölzer, U. (2009). An error propagation prevention method for MIMO-OFDM RLS-DDCE algorithms, *Proc. IEEE International Symposium On Wireless Communication Systems 2009 (ISWCS'09), Siena* pp. 31–35.

Beinschob, P. & Zölzer, U. (2010a). Improving Low-Delay MIMO-OFDM channel estimation, *International ITG Workshop on Smart Antennas 2010*, Bremen, Germany.

Beinschob, P. & Zölzer, U. (2010b). MIMO-OFDM equaliser for spatial multiplexing transmission modes, *Advances in Radio Science* 8: 81–85.
URL: *http://www.adv-radio-sci.net/8/81/2010/*

Bölcskei, H., Gesbert, D. & Paulraj, A. (2002). On the capacity of OFDM-based spatial multiplexing systems, *IEEE Transactions on Communications* 50(2): 225–234.

Chu, D. C. (1972). Polyphase codes with good periodic correlation properties, *IEEE Transactions on Information Theory* 18(4): 531–532.

Dall'Anese, E., Assalini, A. & Pupolin, S. (2009). On the effect of imperfect channel estimation upon the capacity of correlated MIMO fading channels, *IEEE 69th Vehicular Technology Conference, VTC Spring 2009*, pp. 1–5.

Gallager, R. G. (1962). Low-density parity-check codes, *IRE Transaction on Information Theory* 8(1): 21–28.

Gallager, R. G. (1963). *Low Density Parity-Check Codes*, MIT Press, Cambridge, MA.

Glavieux, A., Loat, C. & Labat, J. (1997). Turbo equalization over a frequency selective channel, *Proceedings of the International Symposium of Turbo Codes, Brest, France* pp. 96–102.

Hagenauer, J., Offer, E. & Papke, L. (1996). Iterative decoding of binary block and convolutional codes, *IEEE Transactions on Information Theory* 42(2): 429–445.

Hochwald, B. & ten Brink, S. (2003). Achieving near-capacity on a multiple-antenna channel, *IEEE Transactions on Communications* 51(3): 389–399.

Liu, H., Wang, X. & Xiong, Z. (2003). Iterative receivers for OFDM coded broadband MIMO fading channels, *IEEE Workshop on Statistical Signal Processing* pp. 355–358.

Lozano, A. & Jindal, N. (2010). Transmit diversity vs. spatial multiplexing in modern MIMO systems, *IEEE Transactions on Wireless Communications* 9(1): 186–197.

MacKay, D. (1999). Good error-correcting codes based on very sparse matrices, *IEEE Transactions on Information Theory* 45(2): 399–431.

Proakis, J. G. & Salehi, M. (1994). *Communication Systems Engineering*, Prentice Hall International, Eaglewood Cliffs, New Jersey 07632.

Richardson, T. J., Shokrollahi, M. A. & Urbanke, R. L. (2001). Design of capacity-approaching irregular low-density parity-check codes, *IEEE Transactions on Information Theory* 47(2): 619–637.

Russell, M. & Stuber, G. (1995). Interchannel interference analysis of OFDM in a mobile environment, *IEEE 45th Vehicular Technology Conference, VTC 1995*, Vol. 2, pp. 820–824.

Spatial channel model for Multiple Input Multiple Output (MIMO) simulations (2008). *Technical Report 25.996*, 3rd Generation Partnership Project (3GPP), Technical Specification Group Radio Access Network, 06921 Sophia-Antipolis Cedex, France.

ten Brink, S. (1999). Convergence of iterative decoding, *Electronics Letters* 35(10): 806–808.

ten Brink, S. (2001). Convergence behavior of iteratively decoded parallel concatenated codes, *IEEE Transactions on Communications* 49(10): 1727–1737.

ten Brink, S., Kramer, G. & Ashikhmin, A. (2004). Design of low-density parity-check codes for modulation and detection, *IEEE Transactions on Communications* 52(4): 670–678.

Adaptive Filtering Applications

Edited by Dr Lino Garcia

ISBN 978-953-307-306-4
Hard cover, 400 pages
Publisher InTech
Published online 24, June, 2011
Published in print edition June, 2011

Adaptive filtering is useful in any application where the signals or the modeled system vary over time. The configuration of the system and, in particular, the position where the adaptive processor is placed generate different areas or application fields such as: prediction, system identification and modeling, equalization, cancellation of interference, etc. which are very important in many disciplines such as control systems, communications, signal processing, acoustics, voice, sound and image, etc. The book consists of noise and echo cancellation, medical applications, communications systems and others hardly joined by their heterogeneity. Each application is a case study with rigor that shows weakness/strength of the method used, assesses its suitability and suggests new forms and areas of use. The problems are becoming increasingly complex and applications must be adapted to solve them. The adaptive filters have proven to be useful in these environments of multiple input/output, variant-time behaviors, and long and complex transfer functions effectively, but fundamentally they still have to evolve. This book is a demonstration of this and a small illustration of everything that is to come.

How to reference

In order to correctly reference this scholarly work, feel free to copy and paste the following:

Patric Beinschob and Udo Zolzer (2011). Adaptive MIMO Channel Estimation Utilizing Modern Channel Codes, Adaptive Filtering Applications, Dr Lino Garcia (Ed.), ISBN: 978-953-307-306-4, InTech, Available from: http://www.intechopen.com/books/adaptive-filtering-applications/adaptive-mimo-channel-estimation-utilizing-modern-channel-codes

INTECH
open science | open minds

InTech Europe
University Campus STeP Ri
Slavka Krautzeka 83/A
51000 Rijeka, Croatia
Phone: +385 (51) 770 447
Fax: +385 (51) 686 166
www.intechopen.com

InTech China
Unit 405, Office Block, Hotel Equatorial Shanghai
No.65, Yan An Road (West), Shanghai, 200040, China
中国上海市延安西路65号上海国际贵都大饭店办公楼405单元
Phone: +86-21-62489820
Fax: +86-21-62489821

IntechOpen